VI International Conference on Adaptive Modeling and Simulation
ADMOS 2013
J. P. Moitinho de Almeida, P. Díez, C. Tiago and N. Parés (Eds)

AN ADAPTIVE MESH REFINEMENT ALGORITHM BASED ON ELEMENT SUBDIVISION WITH APPLICATION TO GEOMATERIALS

CLAIRE E. HEANEY[‡], PAUL G. BONNIER[†], RONALD B.J. BRINKGREVE[*†] and MICHAEL A. HICKS[*]

[‡] Cardiff University
Institute of Mechanics and Advanced Materials
Cardiff School of Engineering
Queen's Buildings, The Parade
Cardiff CF24 3AA
Wales, UK
e-mail: claire.e.heaney@gmail.com

[*]Delft University of Technology
Geo-Engineering Section
Stevinweg 1
2628 CN Delft
The Netherlands

[†]Plaxis BV
P.O. Box 572
2600 AN Delft
The Netherlands

Key words: Adaptive Mesh Refinement, Elastoplasticity, Geomaterials

Abstract. The implementation of Adaptive Mesh Refinement (AMR) within the geotechnical software package PLAXIS 2D is described in this paper. A recovery-based algorithm is used which aims to reduce the discretisation error by refining the mesh during the solution process. The error is estimated with a Zienkiewicz-Zhu-type error estimator but based on the incremental deviatoric strain instead of stress. The deviatoric strain field is compared with an improved field calculated by superconvergent patch recovery. Once elements with large errors have been detected, mesh refinement takes place. A combination of regular subdivision and longest-edge bisection is employed. Mapping history variables from the old mesh to the new mesh is accomplished by using the recovered solutions and the shape functions. The AMR algorithm is demonstrated for a biaxial compression test.

1 INTRODUCTION

Adaptive Mesh Refinement (AMR) is a technique which refines a mesh as part of the solution procedure of a boundary value problem. The aim is to achieve the best mesh possible (within certain constraints) for each load level. AMR is applied to problems which have features developing on different scales. In geotechnics, a retaining wall is one such an example. The boundary condition will be applied along the wall which may have a height of the order of metres. Should the load be large enough, a shear band or failure surface may develop in the soil behind the wall with a width of millimetres. In order to properly model the shear band, the elements need to be sufficiently small. For most of the domain this would be a waste of computational effort, and, as the location of the shear band is not known *a priori*, AMR presents as an obvious solution by automatically generating small elements where they are most needed.

AMR works by quantifying the discretisation error in the finite element (FE) solution, and, when the global error norm exceeds a specified tolerance, certain elements are marked for refinement. Once the mesh has been refined and the solution has been mapped to the new mesh, the loading is resumed. This allows the mesh to be refined in regions where the error is high (eg. due to the large strain gradients) resulting in a more accurate description of the shear band.

It has recently been suggested that AMR is not widely used, either in industry (for structural mechanics applications) [1, 2] or in the field of geotechnics [3]. Noteworthy exceptions in geotechnics are [4, 5, 6, 3]. This paper aims to implement a straightforward AMR algorithm which progressively refines the mesh when the global error exceeds a given tolerance.

2 FORMULATION

AMR has been implemented within Plaxis's 2D displacement-based FE solver [7]. Throughout this paper 6-noded triangular elements are used within unstructured meshes. The approximation of the displacements is therefore quadratic. Load or displacement boundary conditions are applied in increments as is usual for materials that behave non-linearly. Once an increment has converged, the AMR algorithm recovers nodal fields and then calculates the error. If the error exceeds the user-defined tolerance, the refinement and mapping algorithms are called. The FE solver then applies the next increment. The four stages of the algorithm are now briefly discussed. A more detailed description can be found in [8].

2.1 Recovery

Variables defined at integration points are recovered at the nodes in order to estimate the error and to facilitate the mapping process. For this purpose, Superconvergent Patch Recovery (SPR) is used [9]. It is an efficient, local method involving the inversion of a relatively small matrix (small when compared to the size of the global stiffness matrix).

The implementation of SPR involves two stages: first, assembling the patches (groups of neighbouring elements) and second, fitting least squares surfaces to the integration point values in each patch. Node-based patches are implemented here, which are formed around each interior vertex node (often referred to as an "assembly node"). The patch is composed of all those elements which contain the assembly node. To recover the solution at nodes on or near the boundary, the standard node-based patches containing elements in contact with the boundary can be extended to include the boundary nodes (as suggested in [10]).

In each patch, a least squares fit is carried out to the data at integration points. In SPR the least squares fit is of the same degree as the displacement shape functions, which are quadratic in this case. Each patch is mapped onto the domain $[-1,1] \times [-1,1]$ to avoid ill-conditioning of the matrix which is inverted to obtain the least squares coefficients.

2.2 Error estimation

Zienkiewicz et. al. [11] prove that their error estimator (described in [12]) is asymptotically exact for linear elastic problems. For elastoplastic problems Boroomand et. al. [13] introduce an error estimator based on incremental energy. More recently Hicks [6] employed an error estimator based upon a measure of incremental deviatoric strain. The incremental shear strain invariant, $\Delta\gamma$, is defined as

$$\Delta\gamma = \sqrt{\Delta\varepsilon_{ij}^{\text{dev}}\, \Delta\varepsilon_{ij}^{\text{dev}}} \,, \tag{1}$$

where $\Delta\varepsilon_{ij}^{\text{dev}}$ is the $_{ij}{}^{\text{th}}$ component of the incremental deviatoric strain tensor. The error in this quantity with respect to the L_2 norm is given by

$$||e||_{\Delta\gamma} = \sqrt{\int_{\Omega} (\Delta\gamma^* - \Delta\gamma)^2 \, d\Omega} \,, \tag{2}$$

where $\Delta\gamma^*$ is the recovered field based on the recovered incremental strains. This estimator should be especially suitable for geomechanical problems which exhibit large changes in strain.

The error estimator for element `iEl` is given by

$$||e||_{\Delta\gamma}^{\texttt{iEl}} = \sqrt{\int_{\Omega_{\texttt{iEl}}} (\Delta\gamma^* - \Delta\gamma)^2 \, d\Omega} \,, \tag{3}$$

and from this, the global error norm can then be calculated:

$$||e||_{\Delta\gamma} = \sqrt{\sum_{\texttt{iEl}=1}^{\texttt{nEl}} \left(||e||_{\Delta\gamma}^{\texttt{iEl}}\right)^2} \,. \tag{4}$$

Either of the above error measures can be made relative by dividing by

$$||\Delta\gamma^*|| = \sqrt{\int_\Omega (\Delta\gamma^*)^2 \, d\Omega} \; . \tag{5}$$

Both local and global errors are used in this implementation of AMR. The global estimate is compared against a user-defined tolerance, and, if it exceeds the tolerance, mesh refinement is triggered. The local (or element) error indicates which elements should be refined. The approach followed here is to link the user-defined global tolerance with the local, element scale to provide a local tolerance. This method relies on the concept of an optimal mesh where the error is equally distributed over the elements (for example [14]). Given a user-defined global tolerance η (which is a relative measure), the condition for triggering refinement is

$$\frac{||e||_{\Delta\gamma}}{||\Delta\gamma^*||} \geqslant \eta \; . \tag{6}$$

Introducing the assumption that the local errors are equally distributed over the mesh gives

$$||e||_{\Delta\gamma}^{\text{local}} \geqslant \frac{\eta \, ||\Delta\gamma^*||}{\sqrt{\texttt{nEl}}} \; , \tag{7}$$

where `nEl` is the total number of elements. So, once the global error exceeds the user-defined (global) tolerance, then all elements whose error exceeds $\frac{\eta \, ||\Delta\gamma^*||}{\sqrt{\texttt{nEl}}}$ will be marked for refinement.

2.3 Mesh Refinement

There are two ways of refining a mesh in $h-$adaptivity: by regeneration or by subdivision. Regeneration is often used and produces elegant-looking meshes directly indicative of the underlying physical mechanism. However, once the mesh has been regenerated, the solution must be mapped from the old mesh to the new mesh throughout the entire domain. In order to limit the numerical diffusion which may occur as a result of transferring the solution between meshes, and to be more efficient, subdivision is used. Here the transfer of the solution is carried out only within elements which have been refined. One way to subdivide elements is to use regular bisection. This refers to the splitting of an element into four elements by joining the midpoints of the triangle's edges [15]. Between a regularly-refined element and a non-refined element will be a non-conforming edge with hanging nodes. A straightforward solution to this is adopted here based on Rivara's longest-edge bisection method [16]. It is applied to any elements which, after being regularly refined, have non-conforming edges. This procedure is repeated until the mesh is conforming.

2.4 Mapping

New elements require values of displacement and stress, and also any state variables which are associated with the constitutive model. Displacements can be mapped using the shape functions and the nodal values of displacement. In order to map the stresses, they are first recovered at the nodes using SPR. Then they can be mapped to the new mesh just as the displacements were. Any integration-point values can be mapped using this method. After mapping, the stress field will no longer be in equilibrium with the applied force. A zero-load increment can be applied in order to resolve this, if necessary.

3 RESULTS

A drained biaxial compression test was simulated to demonstrate the performance of the AMR algorithm. The geometry and boundary conditions can be seen in Figure 1, where L, the width of the sample, is used to normalise the computed displacements. The constitutive model is linear elastic, perfectly plastic with a Mohr-Coulomb yield criterion and associated flow. The parameters are Young's Modulus $E = 10\,\text{MPa}$, Poisson's ratio $\nu = 0.2$, friction angle $\phi = 30°$ and cohesion $c = 5.5\,\text{kPa}$. Vertical displacement increments are applied to the top boundary along which horizontal displacement is prevented. The base is fully fixed.

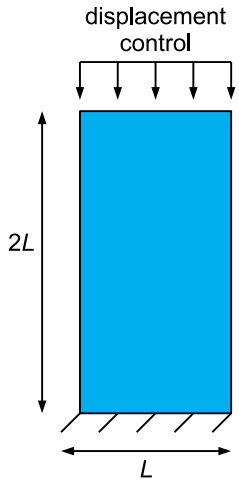

Figure 1: The biaxial test modelled in plane strain, with a fully fixed base and a displacement control through a rough and rigid end plateau.

First, the biaxial problem was simulated with the standard FE method using a fixed mesh (ie. with no adaptivity). Six-noded triangular elements were used. The global error norm was calculated based on the incremental deviatoric strain estimator defined in Section 2.2. The behaviour of the estimator can be seen in Figure 2 for a fixed mesh of 270 elements of approximately equal size. The error increases extremely rapidly during steps 4 to 7. As can be seen from Figure 4, this corresponds to the approach to the peak

of the load-displacement curve as the solution becomes non-homogeneous. The global error norm then reduces until around step 20, after which it remains constant. The global error norm controls when adaptive remeshing is triggered and is therefore crucial to the refinement process. This plot would suggest that the incremental deviatoric strain estimator is a suitable measure as it is able to identify the onset of localisation which occurs as the peak in the load-displacement curve is approached.

An AMR simulation was then carried out, starting from a mesh of 270 elements with a global error tolerance of 2.5%. Figure 3 shows the global error norm in this case, with the broken horizontal line representing the global error tolerance. The filled circles indicate a step which ends with refinement. It can be seen that refinement is initiated four times in the vicinity of the peak of the load-displacement curve, at step numbers 4, 5, 6 and 10. (At the end of the simulation, the error exceeds the tolerance; however, as over 95% of the displacements have already been applied, refinement is not allowed.)

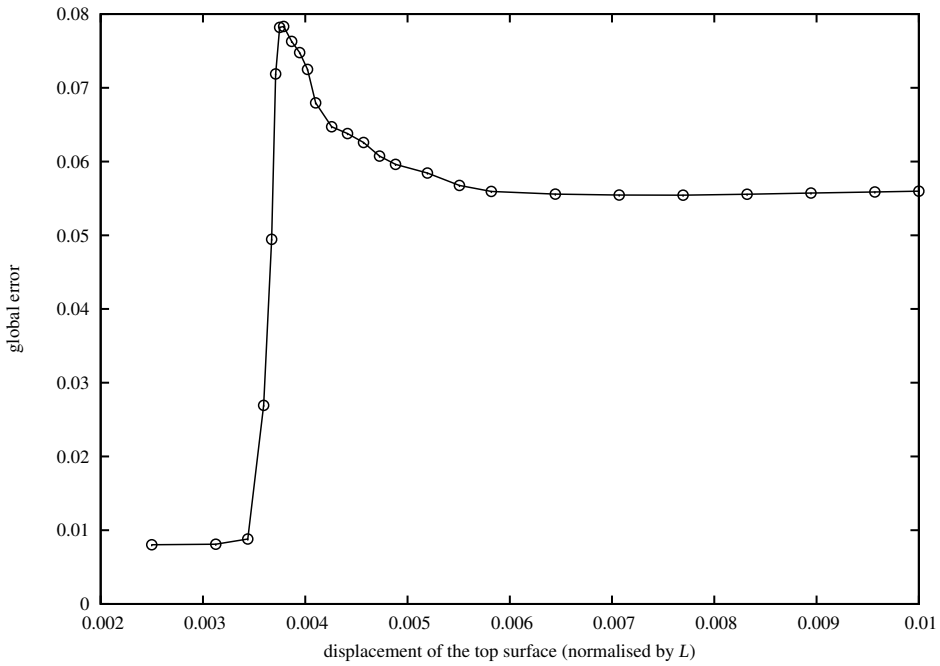

Figure 2: The global error norm using the error estimator based on the incremental deviatoric strain plotted against the normalised displacement boundary condition.

Load-displacement curves are plotted in Figure 4. Curves from two fixed-mesh simulations are shown for comparison, these using 142 and 4162 elements. The AMR results agree extremely well with the results from the finest fixed mesh, the load-displacement curves being almost coincident. The steps which trigger refinement are indicated by hollow circles. The load-displacement curve for the AMR simulation remains smooth despite the mesh refinement.

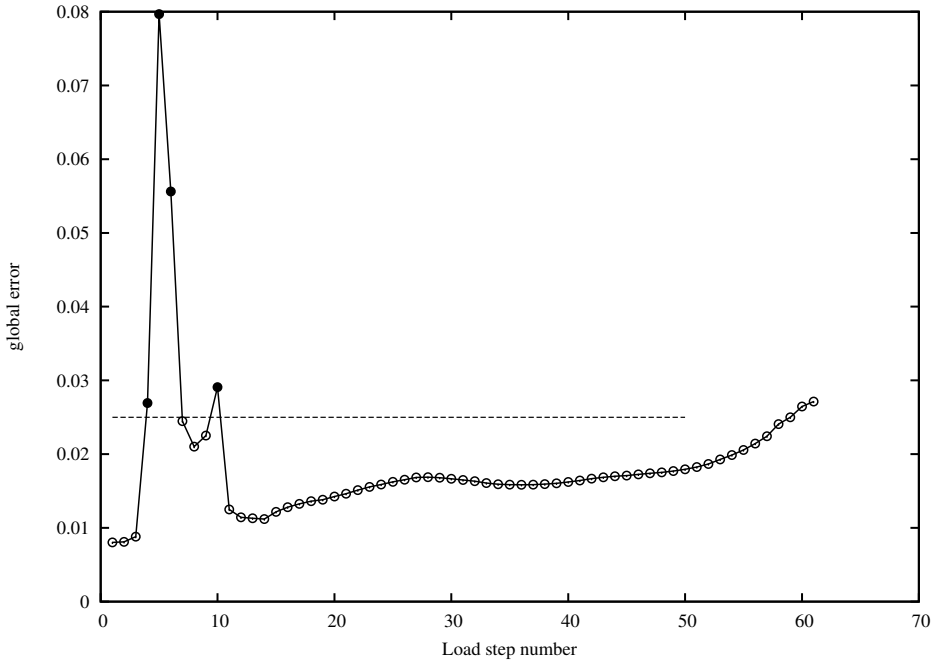

Figure 3: The global error norm plotted against the number of (load) steps during adaptive mesh refinement. Filled circles indicate when refinement is triggered.

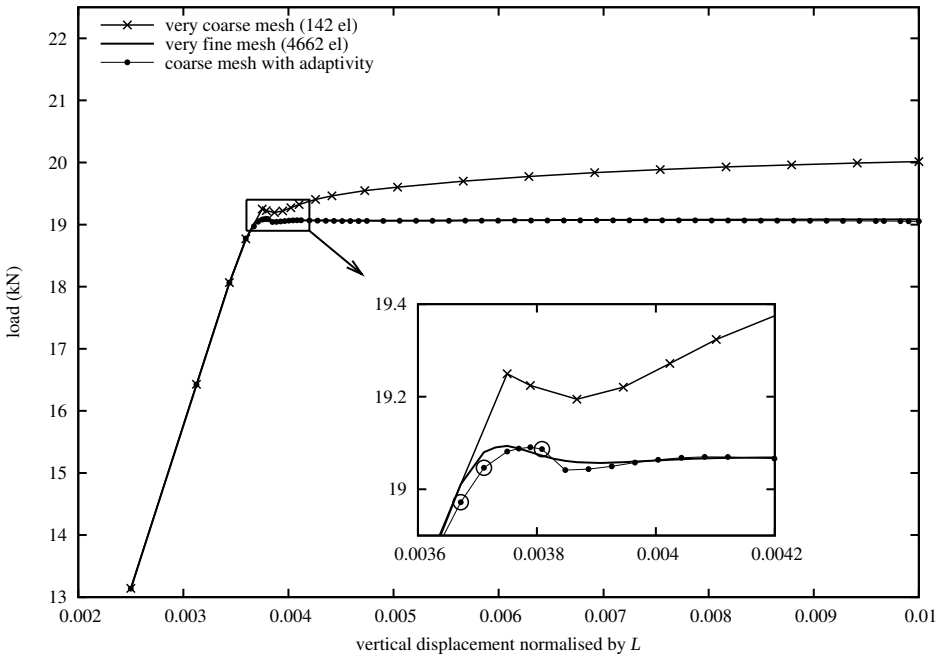

Figure 4: Load-displacement curves for the AMR simulation and for two standard FE simulations with fixed meshes.

Finally, Figure 5 shows plots of the incremental shear strain invariant ($\Delta\gamma$) at the end of the simulation. The results agree well with the analytical prediction for the inclination of the shear band (ϑ). According to Roscoe [17], this is given by $\vartheta = \pi/4 + \psi/2$ where ψ is the dilation angle (in radians).

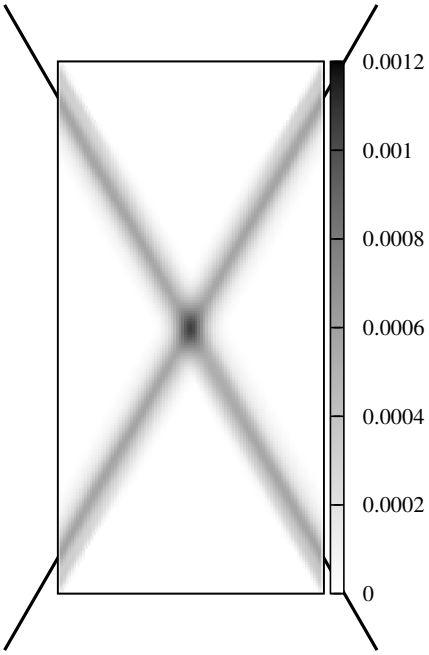

Figure 5: A contour map of the incremental deviatoric strain ($\Delta\gamma$) at the final step for the AMR algorithm. The black lines indicate the inclination of the shear band as predicted by Roscoe.

4 CONCLUSIONS

An AMR algorithm has been implemented in Plaxis 2D. Results are shown for a biaxial compression test. The implementation is recovery based and uses element subdivision rather than mesh regeneration when refinement is required. The adaptive algorithm triggers relatively few refinement steps but is nevertheless effective due to the success of the incremental error estimator in pinpointing the onset of localisation. The load-displacement curve is smooth despite the mesh refinement. This would suggest that the transfer of data from the old to the new mesh is carried out effectively. The inclination of the shear band from the numerical results agrees very well with the analytical prediction given by Roscoe.

Acknowledgments

The authors gratefully acknowledge the support of GEO-INSTALL: a project funded by the European Community through the Marie Curie IAPP programme (Contract No. PIAP-GA-2009-230638). The first author's attendance at ADMOS is funded by Cardiff School of Engineering under EPSRC grant number EP/J01947X/1EP/J01947X/1.

REFERENCES

[1] Pashley, D. Adaptive Re-meshing in Structural Analysis - Part 1. *Benchmark (NAFEMS publication)* (April, 2011) 11-12.

[2] Pashley, D. Adaptive Re-meshing in Structural Analysis - Part 2. *Benchmark (NAFEMS publication)* (October, 2011) 11-13.

[3] Kardani, M. and Nazem, M. and Abbo, A.J. and Sheng, D. and Sloan, S.W. Refined h-adaptive FE procedure for large deformation geotechnical problems. *Comput. Mech.* (2012) **49**:21-33.

[4] Perić, D. and Hochard, Ch. and Dutko, M. and Owen, D.R.J. Transfer operators for evolving meshes in small strain elasto-plasticity. *Comput. Methods Appl. Mech. Engrg.* (1996) **137**:331–344.

[5] Hu, Y. and Randolph, M.F. H-adaptive FE analysis of elasto-plastic non-homogeneous soil with large deformation. *Comput. Geotech.* (1998) **23**:61–83.

[6] Hicks, M.A. Coupled computations for an elastic-perfectly plastic soil using adaptive mesh refinement. *Int. J. Numer. Anal. Meth. Geomech.* (2000) **24**:453–476.

[7] Brinkgreve, R.B.J. and Swolfs, W.M. and Engin, E. *Plaxis 2D 2011* (2011).

[8] Heaney, C.E. and Bonnier, P.G. and Brinkgreve, R.B.J. and Hicks, M.A. Adaptive Mesh Refinement with application to geomaterials. *In preparation for submission to Comput. Geotech.* (2013)

[9] Zienkiewicz, O.C. and Zhu, J.Z. The superconvergent patch recovery and *a posteriori* error estimates. *Int. J. Numer. Meth. Engng.* (1992) **33**:1331–1364.

[10] Zienkiewicz, O.C. and Zhu, J.Z. Superconvergence and the superconvergent patch recovery. *Finite Elem. Anal. Des.* (1995) **19**:11–23.

[11] Zienkiewicz, O.C. and Zhu, J.Z. The superconvergent patch recovery (SPR) and adaptive finite element refinement. *Comput. Methods Appl. Mech. Engrg.* (1992) **101**:207–224.

[12] Zienkiewicz, O.C. and Zhu, J.Z. A simple error estimator and adaptive procedure for practical engineering analysis. *Int. J. Numer. Meth. Engng.* (1987) **24**:337–357.

[13] Boroomand, B. and Zienkiewicz, O.C. Recovery procedures in error estimation and adaptivity. *Comput. Methods Appl. Mech. Engrg.* (1999) **176**:127–146.

[14] Mar, A. and Hicks, M.A. A benchmark computational study of finite element error estimation. *Int. J. Numer. Meth. Engng.* (1996) **39**:3969–3983.

[15] Bank, R.E. and Sherman, A.H. and Weisser, A. Refinement algorithms and data structures for regular local mesh refinement. *Scientific computing (IMACS Transactions).* (1983) 3–17.

[16] Rivara, M.C. Design and data structures of a fully adaptive multigrid finite element software. *ACM Transactions on Mathematical Software.* (1984) **10**:242–264.

[17] Roscoe, K.H. The influence of strains in soil mechanics. *Géotechnique* (1970) **20**:129–170.